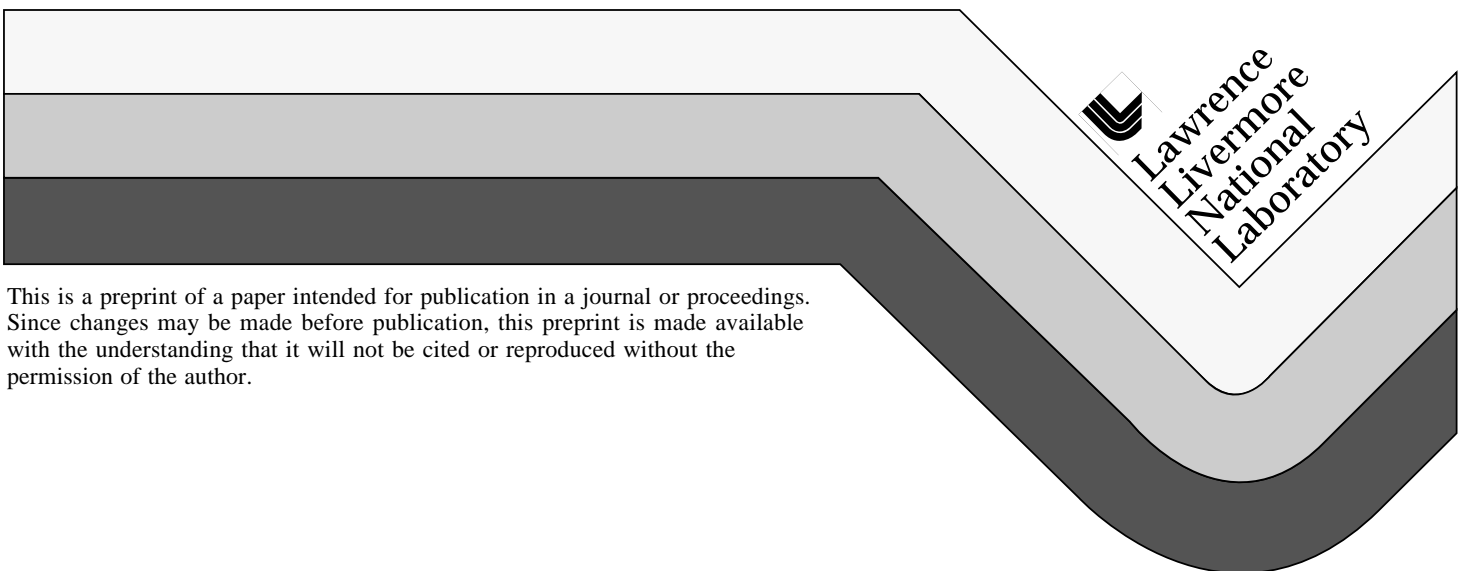


# An Imaging White Light Velocimeter

D. Erskine  
N.C. Holmes

This paper was prepared for submittal to the  
*Optical Society of America Annual Meeting*  
*Rochester, NY*  
*October 20-25, 1996*

October 1996



This is a preprint of a paper intended for publication in a journal or proceedings. Since changes may be made before publication, this preprint is made available with the understanding that it will not be cited or reproduced without the permission of the author.

#### DISCLAIMER

This document was prepared as an account of work sponsored by an agency of the United States Government. Neither the United States Government nor the University of California nor any of their employees, makes any warranty, express or implied, or assumes any legal liability or responsibility for the accuracy, completeness, or usefulness of any information, apparatus, product, or process disclosed, or represents that its use would not infringe privately owned rights. Reference herein to any specific commercial product, process, or service by trade name, trademark, manufacturer, or otherwise, does not necessarily constitute or imply its endorsement, recommendation, or favoring by the United States Government or the University of California. The views and opinions of authors expressed herein do not necessarily state or reflect those of the United States Government or the University of California, and shall not be used for advertising or product endorsement purposes.

# An Imaging White Light Velocimeter

David J. Erskine and Neil C. Holmes

*Lawrence Livermore National Laboratory, PO Box 808, Livermore CA 94550*

An imaging white light velocimeter consisting of two image superimposing Michelson interferometers in series with the target interposed is demonstrated. Interferometrically measured 2-dimensional velocity maps can be made of moving surfaces using unlimited bandwidth incoherent and extended source-area lamps. Short pulse and broadband chirped pulse lasers can be used to provide temporal resolution not previously possible with monochromatic illumination. A  $\sim 20$  m/s per fringe imaging velocimeter is demonstrated using an ordinary camera flash for illumination.

The interferometric measurement of velocities through the Doppler shift of reflected waves is an important and widespread diagnostic tool. Until recently, these velocimeters were restricted to the use of monochromatic illumination so that the Doppler shift was larger or of the same order as the illumination bandwidth. Recently, we presented<sup>1</sup> a method we call white light velocimetry that allows the use of an arbitrary source, including unlimited bandwidth incoherent illumination, and non-collimated beams (lamps having extended emitting areas). Short pulse and chirped pulse lasers can be used for the first time to perform time-resolved velocity interferometry.

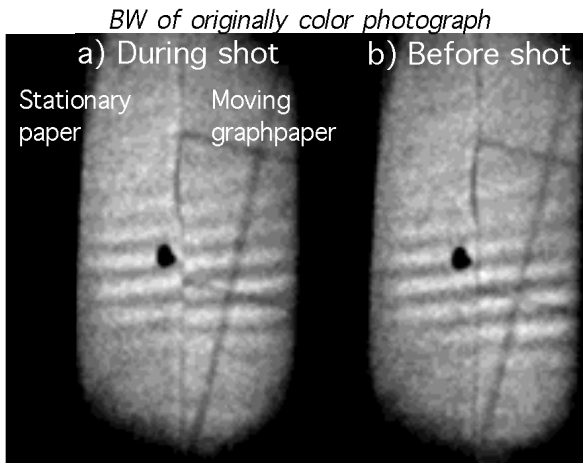


**Fig. 1.** Grayscale representation of multi-color fringes produced by the white light velocimeter prior and during a shot. The fringes were recorded on Kodak Royal 1000 color film. The illumination source was small camera flash of 20  $\mu$ s duration. The target was a stationary piece of paper (left side with dot) overlapping non-uniformly moving graph paper behind it (right side with blue grid lines). This demonstrates the imaging capability, the use of non-collimated white light, and the recording of a non-uniformly moving target. a) The target during the shot; b) The target prior to the shot when both surfaces are

stationary. The fringes on the graphpaper side have shifted vertically due to velocity.

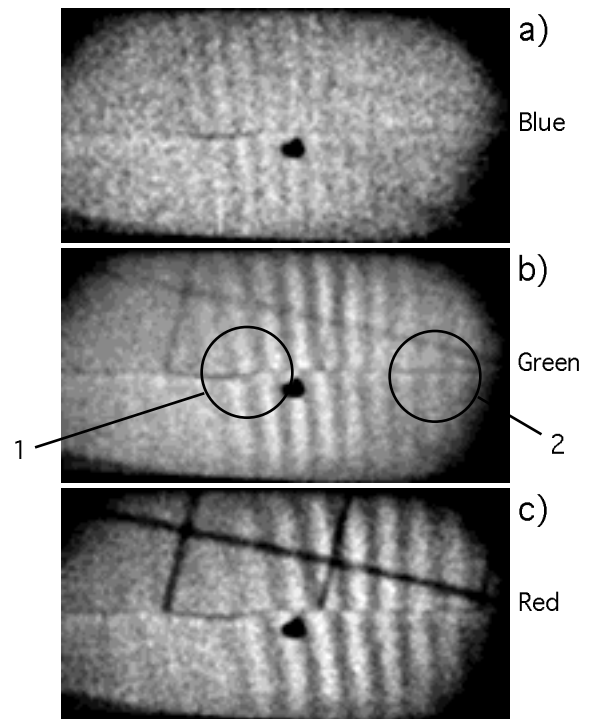


**Fig. 2.** The red, green and blue components of the color photograph discussed in Fig. 1, for the shot. The fringe comb spacing is proportional to average wavelength of sensitivity for the given film emulsion component. The fringe shift at position 1 is approximately 1/2 and at position 2 approximately unity. Analysis shows the velocity increasing from 3 m/s to 20 m/s from left to right side of the image. Uncompensated interferometer dispersion causes the center of the fringe pattern to differ for different colors. The fringe contrast is poorer for blue because the spherical mirror coating is not ideally reflective, causing the interferometer arms to have unequal intensities for blue.

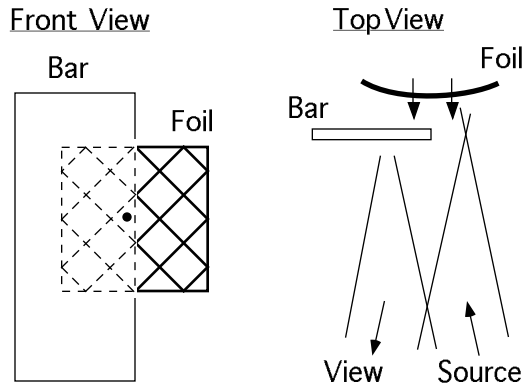


**Fig. 3.** Target configuration. Target was a ~25 mm square aluminum foil propelled by a spark behind its center toward a stationary bar. A white piece of graph paper with 1/4 inch (6.4 mm) blue grid was glued to foil front. White paper was glued to front of the bar and a small dot indicated the approximate axis of spark. The viewing interferometer saw both the stationary and moving surfaces in the image. The moving surface was clamped more strongly at the top edge, resulting in non-uniform motion.

The use of broadband illumination allows unambiguous determination of the zeroth fringe, so that the fringe phase can be tracked through discontinuous velocity histories, such as found in the measurement of shock waves. It produces optimal resolution of debris having different velocities but overlapped in view of the detector, such as debris from a disintegrating target or ground clutter in radar. For targets which can have an unanticipated or evolving albedo spectrum, broadband illumination increases the likelihood of a reflected signal of significant intensity. Femtosecond pulses can be used to provide time resolution. Or, the use of chirped illumination with a diffraction grating on output creates an all-optical streak camera capable of measuring motion over a line image with picosecond resolution<sup>2</sup>. Finally, the white light velocimeter allows the use of incoherent sources which are attractive for their convenience, compactness, cost or large total energy for illuminating a wide area.

Figure 1 and Fig. 2 are the grayscale and color component representations of a color photograph recording the multicolor fringes produced by the white light velocimeter prior and during a shot. Figure 3 shows the target consisting of stationary and moving sheets of white paper. Since they are recorded in the same field of view, as a whole this is a discontinuous non-uniformly moving target. In addition, the moving portion has a velocity which varies continuously, because one edge of the surface was more strongly clamped than the opposite edge. Analysis of red, green, and blue fringe shifts indicates the velocity grows from 3 m/s to 20 m/s from the left to right of Fig. 2. The illumination source was a small camera flash. Conventional velocimetry is with laser illumination and is non-imaging, measuring velocity at a single point, or at most along a line. This experiment is notable because it demonstrates the imaging capability,

the use of wideband incoherent and non-collimated source of light, and the recording of a target whose velocity changes across its surface.

Figure 4 is a line diagram depicting the white light velocimeter (WLV) method. Two nearly delay-matched image superimposing interferometers are used in series with the target interposed. The interferometers are labeled "source" and "viewing", and have delays  $\tau_1$  and  $\tau_2$ , respectively. The superimposing condition requires that for a given interferometer, all images created by the interferometer superimpose longitudinally, transversely and in magnification, even though there is a temporal delay between the rays. This produces an interferometer delay which is independent of ray angle, for each image pixel. The condition of image superposition distinguishes our device from other two-interferometer devices<sup>3</sup> and allows the use of non-collimated broadband sources and the imaging ability.

The two interferometers can either be distinct, as in this demonstration, or can be realized by the same optics if the illumination retro-reflects from the target, as demonstrated in Ref. 1. The latter configuration is the simplest because the delays  $\tau_1$  and  $\tau_2$  are automatically matched. However, separate interferometers may be desired to eliminate glare from shared optics so that weak reflectors can be observed, and so that one interferometer can be aligned differently than the other to form a fine fringe comb across the target image.

If the delays  $\tau_1$  and  $\tau_2$  approximately match within the coherence length of the source, then partial fringes are formed whose phase depends on  $(\tau_1 - \tau_2)$ . Let  $\tau \equiv \tau_1 \approx \tau_2$  be the gross delay value. The velocity per fringe sensitivity  $\eta$  is given approximately by

$$\eta = \langle \lambda \rangle / (2\tau) \quad (1)$$

where  $\langle \lambda \rangle$  is the average wavelength of the light being detected. Equation (1) is used to choose the general size for  $\tau$ , which can range from 1 mm to 10 meters for applications ranging from plasma physics to windtunnel diagnostics.

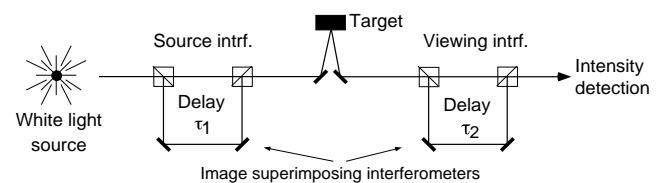


**Fig. 4.** Line diagram of a white light velocimeter. The parallelograms represent generic image superimposing interferometers. If interferometer delays  $\tau_1$  and  $\tau_2$  match within a coherence length of the source, partial fringes are produced at the output which vary with  $(\tau_1 - \tau_2)$ . Target velocity scales the apparent value of  $\tau_1$  due to the Doppler effect, changing the fringe phase.

The production of fringes can be explained either in the time domain, as in Ref. 1, or in the frequency domain, as is done here. Consider each interferometer to be a comb filter with sinusoidal pass bands periodically

spaced  $1/\tau$  apart, in frequency space. The target velocity through the Doppler effect causes the source interferometer comb spectrum to scale by a factor  $(1+2v/c)$ , where  $v$  is the target velocity for normal incidence and  $c$  is the speed of light. As the velocity changes, the overlap between the two slightly different comb filters produces fluctuations in the intensity passing through both interferometers, integrated over the range of wavelengths detected. This is analogous to moiré fringes from two overlaid meshes having slightly different pitches.

For Michelson superimposing interferometers, the time averaged output intensity  $\langle I \rangle$  from the viewing interferometer in the region of fringes varies approximately sinusoidally above a constant background as

$$\Delta \langle I \rangle \propto \cos \left[ \frac{2\pi}{\langle \lambda \rangle} c(\tau_1 - \tau_2) - \frac{2\pi}{\langle \lambda \rangle} (c\tau_1) \left( \frac{2v}{c} \right) + \phi_0 \right] \quad (2)$$

where  $\Delta \langle I \rangle$  is the fluctuating part of the time averaged intensity, and  $\phi_0$  is some phase constant. The average wavelength is often determined by the detector. For example, in our case by the sensitivity spectra of the red-, green- or blue- emulsions in color film.

A single channel wideband detector could be used to record intensity. However, it is preferable to use a multi-channel detecting system where channels are organized either by wavelength or delay difference ( $\tau_1 - \tau_2$ ). Both methods are used in this demonstration. By slightly misaligning an interferometer mirror, the delay difference is made to vary across the image. Then target velocity causes the fringe comb to displace transversely across the image. In addition to this, the use of color film creates a 3-channel recording organized by wavelength.

Alternatively, a grating could be used to diffract a line or point image into a spectrum. Equation (2) indicates that fringes will be observed versus  $1/\langle \lambda \rangle$ . When this configuration is used with a chirped pulse, a correspondence is made between wavelength and time at the target. This forms an optical streak camera<sup>2</sup> which measures velocity history along a line across the target.

The interferometers can be of a Michelson class (generating two images) or Fabry-Perot class (infinite series of images of decreasing intensity). Monochromatic superimposing Michelson interferometers achieved by an etalon in one arm have been used in VISAR velocity interferometers for many years<sup>4</sup>. These satisfy the superimposing condition only for one wavelength due to dispersion in the etalon and thus are unsuitable for a WLW. An example of a non-superimposing interferometer is the conventional Fabry-Perot, which longitudinally displaces the successive output rays for a given input ray. A Fabry-Perot can be made superimposing by adding a positive lens internal to the cavity so that there is exactly +1 magnification per round trip.

The achromatic superimposing Michelson interferometer used in this demonstration uses a relay lens system in one arm. This is shown in Fig. 5, except that a transmissive lens  $L_2$  represents a spherical mirror actually

used. The interferometer delay is given by the path length difference between the two arms. Lenses  $L_2$  and  $L_1$  image the surface of a spherical reflector  $RM_1$  to a so-called apparent mirror surface. This must superimpose with the image of  $M_1$  seen in the beamsplitter BS, and which is called the principal plane. The goal of the interferometer is to superimpose the apparent mirror and principal plane surfaces for a wide range of incident ray angles, positions and wavelengths. Other lenses, not shown, relay the principal plane to the target.

The interferometers of our apparatus have 4 meter delays so that the velocity per fringe proportionality for white light is about 20 m/s. This allows the use of low velocity targets safe for tabletop demonstrations.

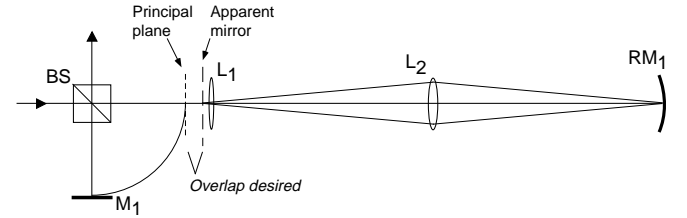


**Fig. 5** A Michelson superimposing interferometer. In actuality, an equivalent spherical reflector is substituted for  $L_2$ . The principal plane is the reflection of  $M_1$  seen in the beamsplitter BS. The apparent mirror surface is the surface of spherical reflector  $RM_1$  imaged by  $L_2$  and  $L_1$ . To achieve full WLW capabilities, the apparent surface should overlap the principal plane for as many input ray angles, positions and wavelengths as possible.

## Acknowledgments

This research was performed under the auspices of the U.S. Department of Energy by the Lawrence Livermore National Laboratory under contract W-7405-Eng-48.

## References

1. D.J. Erskine and N.C. Holmes, "White-light Velocimetry", *Nature* **377**, 317-320 (1995); Errata: the sentence one paragraph above Eq. (2) should read "In general, there is no restriction on the design of either interferometer provide they individually superimpose images created by each arm longitudinally, transversely and in magnification."
2. A simple argument estimates the time resolution of a chirp illuminated streak system to be
 
$$\Delta t = \sqrt{\frac{T_p}{f_2 - f_1}}$$
 where  $T_p$  is the pulse duration having a range of frequencies  $f_1$  to  $f_2$ .
3. S. Gidon and G. Behar, "Multiple-line laser Doppler velocimetry", *Appl. Opt.* **27**, 2315-2319 (1988).
4. W. Hemsing, "Velocity sensing interferometer (VISAR) modification", *Rev. Sci. Instrum.* **50**, 73-78 (1979).

*Technical Information Department • Lawrence Livermore National Laboratory*  
*University of California • Livermore, California 94551*

